Finite Element Analysis of an Energy Absorbing Sub-floor Structure

Scott C. Moore

Benson Dexter

Abstract

As part of the Advanced General Aviation Transportation Experiments program, the National Aeronautics and Space Administration's Langley Research Center is conducting tests to design energy absorbing structures to improve occupant survivability in aircraft crashes. An effort is currently underway to design an energy absorbing (EA) sub-floor structure which will reduce occupant loads in an aircraft crash. However, a recent drop test of a fuselage specimen with a proposed EA sub-floor structure demonstrated that the effects of sectioning the fuselage on both the fuselage section's stiffness and the performance of the EA structure were not fully understood. Therefore, attempts are underway to model the proposed sub-floor structure on computers using the DYCAST finite element code to provide a better understanding of the structure's behavior in testing, and in an actual crash.

Introduction

The National Aeronautics and Space Administration (NASA), the Federal Aviation Administration (FAA), and several aircraft and avionics manufacturers are currently working in partnership to develop new technologies for use in future general aviation and commuter aircraft. This goal of this research, known as the Advanced General Aviation Transportation Experiments (AGATE), is to revitalize the general aviation and commuter aircraft industry in the United States. There are four major NASA work packages comprising the general aviation element of AGATE: Integrated Cockpit Systems, Propulsion, Sensors, and Controls, Integrated Design and Manufacturing, and Icing Protection Systems. The goal of the Integrated Design and Manufacturing package is to develop lighter, safer, and more affordable certified aircraft structural concepts.

Current Research

NASA Langley Research Center (LaRC) has been conducting impact dynamics research and full scale crash testing for over 20 years. In recent years, NASA impact dynamics research has concentrated more and more on composite materials, which will be used much more extensively in aviation in the future. As part of the Integrated Design and Manufacturing work package of AGATE, LaRC is conducting research into energy absorbing (EA) structures for use in next generation general aviation aircraft. NASA recently acquired two seven seat Learfan aircraft with carbon composite fuselages. One of the aircraft, with the standard metal beam floor structure, was outfitted with energy absorbing seats, side by side with standard FAA Part 132 9g aircraft seats, and crash tested at LaRC's Full Scale Impact Dynamics Research Facility (IDRF) to form a baseline for future tests. At impact, the aircraft was traveling at 31 fps vertical velocity

and 81 fps longitudinal velocity. The maximum vertical accelerations measured in the seat pans were approximately 80g in the standard seats and 40g in the EA seats, compared with the human tolerance level of 50g. However, the test dummies in the EA seats sustained spinal loads of 1600 lbs, above the maximum human tolerance of 1500 lbs. These results demonstrate that, even in a moderate impact such as this one, occupants in EA seats would likely suffer severe injuries or death and occupants in standard 9g aircraft seats would almost certainly be killed.

The next stage in testing is to replace the standard sub-floor structure with an energy absorbing structure and repeat the test. However, before this can occur, a suitable sub-floor structure has to be developed and tested. One structure currently under consideration is a box core flat-faced composite beam. The structure consists of a 0/90 degree fiberglass core with a skin of +/- 45 degree Kevlar for structural integrity and is filled with rigid closed cell PVC foam. The structure, which has achieved a sustained crushing load of 240 lbf per inch length in dynamic testing is mounted directly under standard T-section seat rails. Recently, this structure was installed and tested in a 36 inch long full scale fuselage section from a Learfan aircraft. EA beams were mounted directly to the fuselage and seat rails under standard 9g aircraft seats, which carried standard instrumented crash dummies. The fuselage section was then drop tested in the IDRF's Vertical Testing Apparatus at 30 fps vertical velocity. However, the EA beams did not crush as anticipated.

After the test, some differences between this test and previous tests in metal fuselage aircraft which may have contributed to the problem were uncovered. Because, in this composite fuselage test, the EA beams were attached directly to the fuselage and there were no lateral beams, the relative stiffness of the fuselage section is more important. Also, the stiffness of the fuselage section was later determined to be less than that of the same section when it is part of the entire fuselage. In addition, the energy absorbing floor beams in the fuselage section act differently from how they would in a full length fuselage. These differences are caused by the shorter lengths of the beams and the differences in restraint at the ends of the beams (both ends of the 36 inch EA beams in the fuselage section test were unrestrained, whereas they would be restrained by the rest of the beam in a full length fuselage). It is therefore important to conduct more research into the effects of varying the lengths of fuselage sections and EA floor beams so that fuselage section drop tests can be both better understood and made more representative of full length aircraft fuselages. Efforts are currently underway to model both the fuselage section and the sub-floor structure on computers. The remainder of this paper focuses on computer modeling of the seat rail and energy absorbing floor beam which together form the sub-floor structure.

Finite Element Modeling

Developing an accurate computer model of the sub-floor structure under consideration is desirable because it would allow simulations to be run without the trouble and expense of a full scale test. Although full scale testing is still needed, these simulations could reveal problems, such as the ones that appeared in the fuselage section test, ahead of time, reducing the need for

costly re-tests. Computer models can also be used to simulate the behavior of materials under many different conditions, reducing the need for actual static and dynamic testing. It is hoped that developing accurate Finite Element Method (FEM) computer models of the sub-floor structure under consideration will lead to a better understanding of the structure and help researchers to recognize and correct potential problems before full scale testing is conducted.

DYCAST (Dynamic Crash Analysis of Structures), the FEM computer code used to model the energy absorbing sub-floor structure is a non-linear structural finite element computer code developed by NASA and Grumman Corporation (Ref. 1). Two different DYCAST elements were used to construct the computer model, the SPNG non-linear spring element and the TSEC beam element. The SPNG element is a non-linear crush spring with energy absorption capability. It's behavior is defined by user-input loading and unloading curves. The TSEC element is a beam element with six different integration points and user-input strain hardening and failure criteria. Each integration point can go plastic or reach failure separately. Also, the stiffness of each integration point is deleted from that of the whole beam when that point reaches the failure criteria (Ref. 1).

Modeling Considerations

For the original model used in the static testing, two sets of nodes were defined, along both the X axis and the line where the ground plane intersects the XZ plane (see Figure 1). Note that the X axis and the ground are 8 inches apart and that both the X and Y axes pass through the centroidal axis of the seat rail. The nodes were initially placed one inch apart in the X direction, along, and directly below the entire length of the beam in consideration. TSEC elements were defined between the elements along the X axis and SPNG elements were defined between these nodes, and the nodes directly below them on the ground. Material properties for 7075-T6 extruded aluminum alloy were used, as well as a 32 point Ramberg-Osgood curve to represent the strain hardening and failure characteristics of the material (see Ref. 2).

Because the cross-section of the seat rail was not identical to that of the TSEC beam, it was necessary to calculate the moment of inertia and centroid of the beam manually. The moment of inertia was then input into DYCAST and the thickness of the DYCAST TSEC flange was varied so that the centroid calculated by DYCAST would be at the proper Z coordinate. These calculations are included in spreadsheet form as Appendix A. The section numbers shown correspond to those in Figure 1. Next, a finite beam on an elastic foundation model was used to verify the DYCAST model (see Ref. 3). The DYCAST springs were made linear with K=7500 lbf per inch deflection and the DYCAST results and elastic foundation results for deflection at the ends and center, and the moment and maximum normal stress at the center were compared at several loads applied at the center node of the model. A comparison with a load of 2000 lbs is included as Appendix B. It was also necessary to construct a load vs. displacement curve for the SPNG elements used in the model. For static modeling, a simple 5 point curve could be used, however, for the dynamic cases, it was necessary to use a 15 point curve to smooth the rapid

changes in slope because of numerical integration problems which would otherwise result. A typical dynamic spring curve representing a sustained crushing load of 240 lbf/in length is included as Figure 2. On this curve, negative displacements and forces represent and cause, respectively, compression. It should be noted that this curve is for springs used with the 1/2 inch length TSEC elements used in some dynamic models, and that the level portion of the graph is slightly less than half of 240 lbf to account for the fact that there is always one more spring than beam element in each model. The static springs have a similar shape, but level off at slightly less than the 200 lbf/in length value used for the static crushing load (1 inch elements).

Static Model

The first series of tests involved static models with 1 inch elements at lengths of 12 and 24 inches, and loads of 2475 lbf and 4800 lbf, respectively. Graphs of the results are included as Figures 3 and 4. Please note that all seat rail displacement graphs represent only the left halves of the structure. The structures are symmetric about the right edge of the graphs. The models were run on a Digital Equipment Corporation Microvax. All nodes were constrained to allow translation in only the Z direction and rotation about only the Y axis. The translation restriction was imposed because of convergence problems with the static integrator. However, in the actual structure, the elements can also translate in the X direction. For this reason, the results are not representative of the actual material behavior. Therefore it was desirable to create a more accurate model.

Dynamic Model 1

In an attempt to more accurately model the behavior of the sub-floor structure, a dynamic model was created. The model was run at eight different lengths, 12 in, 13 in, 14 in, 16 in, 18 in, 22 in, 26 in, and 36 in. on several Sun Sparc 10 series workstations. The 12 through 16 inch models used 1/2 inch length elements, while the 18 through 36 inch models used 1 inch length elements due to a limit DYCAST imposes on the number of elements and the large amount of processor time required for these models. In each case the load was a 104 lbm point mass applied to the center node of the beam. The beam was then given an initial velocity of 30 fps in the negative z direction. In an effort to further reduce the computer time required, the symmetry of the beams used to represent the whole beam by modeling only the left half. To do this, the strength of the center spring was cut in half and a mass of 52 lbm was applied. The center node was then constrained to no rotation to force symmetry. These models were verified by comparing them to their full length counterparts and the results were identical. All of the other nodes along the beam were allowed translate in both the X and Z directions, and to rotate about the Y axis. A large unloading slope, comparable to the initial slope of the SPNG elements, was

used to make the deformation permanent. A Newmark-Beta implicit integration scheme was originally tried, however system energy errors of greater than 1000% resulted. The Wilson-Theta implicit integrator was then tried, and yielded much better results. This integrator was used for all remaining models, and system energy errors were all less than 5% and usually less than 1%.

Graphs of the 12, 13, 14, 18, 26, and 36 inch models at 4 millisecond increments are included as Figures 5 through 10, respectively. Figures 5 through 7 exhibit unusual behavior at the last three time increments. These are a consequence of the rebound the center node experiences when it reaches the very steep slope towards the end of the load vs. displacement curve and the unloading slopes on the springs. Because this behavior is uncharacteristic of the actual material, deflections after the center has reached the point of maximum Z deflection are indicated on the graphs as hairlines. A more troubling trend, however, is the large X deflection of the ends of the beams in all but the 26 inch case. This is not characteristic of the results of dynamic testing conducted at the IDRF. The large deflections occurred because the model does not take in to account the strength added to the structure by the EA beam in directions other than the Z direction. The actual structure also resists crushing in the X direction and the +/- 45 degree Kevlar fibers in the beam give it a strong resistance to torsion. Next, an attempt was made to compensate for these factors.

Dynamic Model 2

In an attempt to compensate for the composite beam's X direction crush resistance and resistance to torsion, springs were attached from the end node of the 13 inch model to a point far in the positive X direction (so that only X and not Z deflections of the beam would affect the length of this new spring). Springs with loading curves identical to those used on each beam were then added and the dynamic tests were re-run in a trial and error process until the final X deflection of the end of the beam was close to that observed in a dynamic test of a 13 inch specimen. Similar beam-end X deflections were observed with 13 springs attached to the end (the equivalent of two springs per inch). The model was then run at lengths identical to those used in Dynamic Model 1 with two springs per inch of model length for 12 to 16 inches, and one spring per inch for 18 to 36 inches (the springs were twice as strong for these lengths due to the 1 inch elements). Plots of the displacements and accelerations of the mass at the center of each beam are included as Figures 11 through 16. Upon comparing the results of the 13 inch model (Figure 12) with a specimen from a dynamic test, it was discovered that the Z displacements along the beam were almost identical. While the X displacements were modeled after those of the test specimen, the fact that the Z displacements along the beam were the same indicates that the vertical springs represent the crushing behavior accurately and that the overall model is accurate for the 13 inch length. It can also be assumed that the models accurately represent the behavior of 14 and 12 inch specimens because they are close in length to the 13 inch model which has been verified. However, further research is necessary to determine if the scheme for adding springs to the end in the longer length models correctly represents the behavior of the material. However, even if it doesn't, corrections should be possible by simply adding or deleting springs.

538

Conclusions

Of the three different types of finite element models attempted, the third one, Dynamic Model 2, has the most promise. It has demonstrated the ability to accurately model the behavior of a test specimen, and with a few more dynamic tests, it could be verified and corrected, if necessary, for other lengths. The Static Model did not accurately represent the behavior of the material, although this is probably because numerical integration problems necessitated limiting the degrees of freedom of the beam beyond what was accurate. However, the static model was useful in that it allowed for verification with elastic foundation theory. Also, Dynamic Model 1 did a poor job of predicting the material behavior because it neglected the stiffness of the energy absorbing beam in other than the Z direction. Although Dynamic Model 2 shows promise, it might also be useful to try and model the sub-floor structure with another more advanced finite element code with the capability to model more complex composite materials. This might provide an even better understanding of the energy absorbing sub-floor structure's behavior.

References

1. Pifko, A. B. and Ogilvie, P. L. DYCAST - A Finite Element Program for the Crash Analysis of Structures. NASA CR 4040, January 1987.

2. Niu, Michael C. Y. I. Airframe Structural Design. Hong Kong: Convilit Press, Ltd., 1993.

3. Hetenyi, M. Beams on Elastic Foundations. Ann Arbor: The University of Michigan Press, 1976.

Appendix A: Moment of Inertia and Centroid Calculations

Seat Track Centroid Calculations

Section	Length In	Width In	Area in^2	Y of Centroid In	Y of Cent.*A In
1			0.07924		0.02861
2			0.23730		0.19652
3			0.02344		0.02087
4			0.03516		0.03296
5			0.03516		0.03296
6			0.04688		0.04980
7			0.04688		0.04980

Sum= 0.49805   Sum= 0.41153

Y Centroid = 0.82629 In

Seat Track Moment of Inertia Calculations

Moments of Inertia about Y' Axis:

Section	Iy'y' In^4
1	0.01490116
2	0.16291523
3	0.01859283
4	0.03094482
5	0.03094482
6	0.05297852
7	0.05297852

Moment of Inertia about Centroid:

$I_{y'y'}$ = 0.36426 In^4

A = 0.49805 In^2

b = 0.82629 In

I_{yy} = 0.02421 In^4

DYCAST Geometry Calculations

Width of Flange (A1) = 2.53125 In
Depth of Web (A2) = 1.00000 In
Thickness of Flange (T1) = In
Thickness of Web (T2) = 0.09375 In

Current Centroid = 0.82621 In

Desired Centroid = 0.82629 In

NOTE: These values do not represent the actual geometry of the
seat rail. They are only dummy values used by DYCAST
to determine the centroid of the seat rail.

Figure 1: DYCAST Model Geometry

Appendix B: Comparison of DYCAST Results with Elastic Foundation Model

Finite Beam on Elastic Foundation Model

Model Geometry:

=E
=Iyy
=b
=K
=P
=L

0.287941 =BETA

Output:

-0.00466 =DEFLECTION AT ENDS (In)   DYCAST=   ERROR= 2.34%

0.045316 =DEFLECTION AT CENTER (In)   DYCAST= 0.044262   ERROR= 2.35%

1881.05363 =MOMENT AT CENTER (In*Ib)   DYCAST= 1792.4   ERROR= 4.71%

64200.5701 =MAX NORMAL STRESS (psi)   DYCAST= 62399
49000 =YIELD STRESS   ERROR= 2.81%

Figure 2: Load vs. Displacement Curve for DYCAST Springs

Figure 3: DYCAST Analysis of Seat Rail under Vertical Static Loading
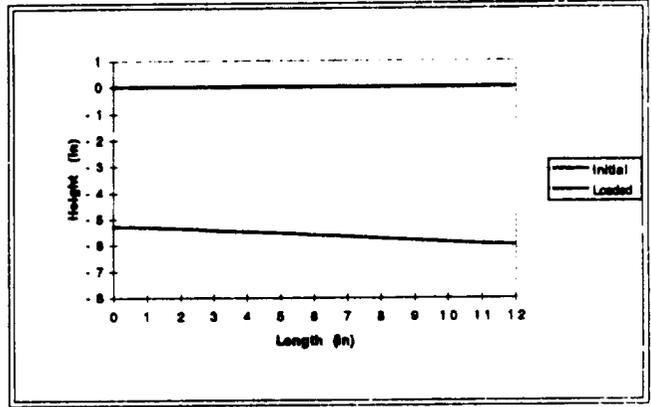Length = 12 in. Load = 2475 Lbs.

Figure 4: DYCAST Analysis of Seat Rail under Vertical Static Loading
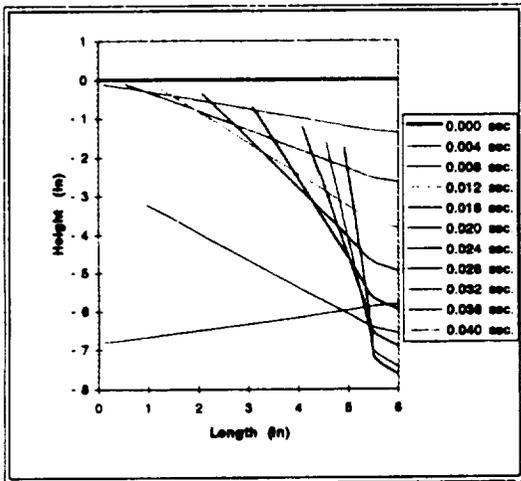Length = 24 in. Load = 4800 Lbs.

Figure 5: DYCAST Analysis of Seat Rail under Vertical Dynamic Loading
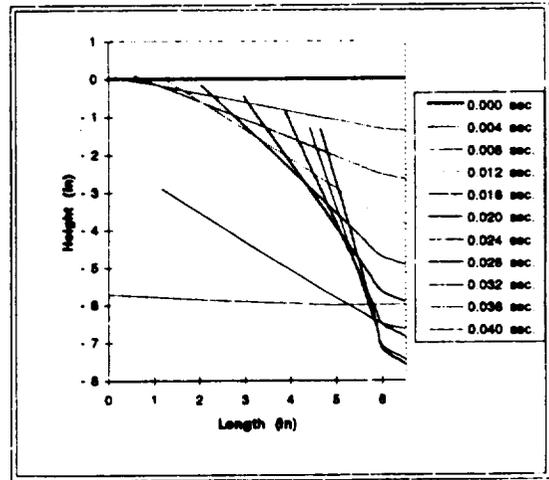Length = 12 in. Load = 104 lbm at 30 fps.

Figure 6: DYCAST Analysis of Seat Rail under Vertical Dynamic Loading
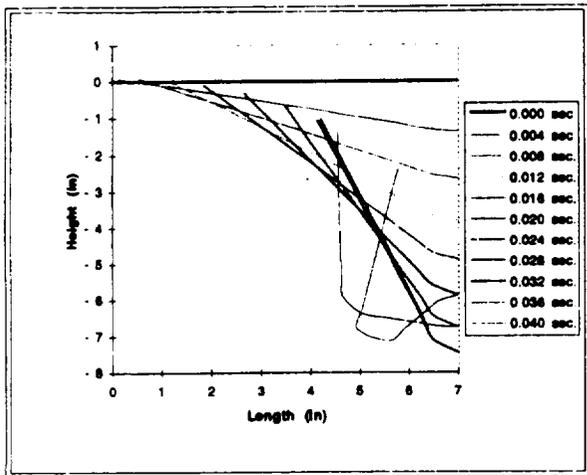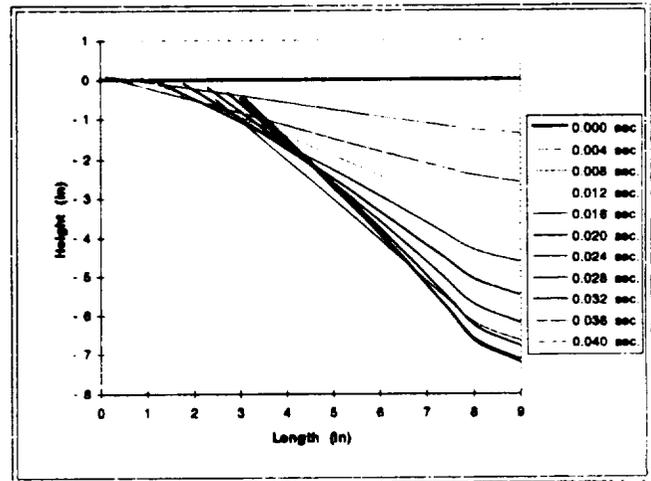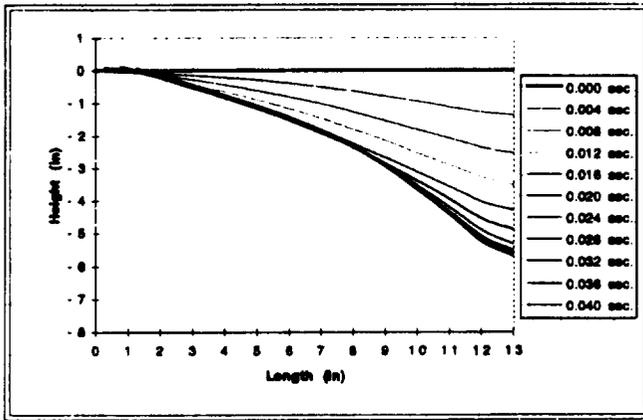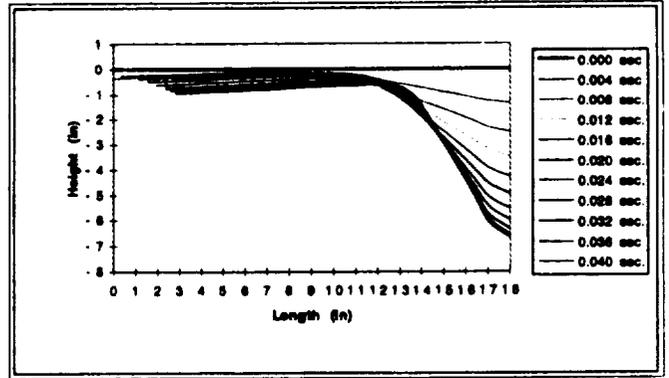Length = 13 in. Load = 104 lbm at 30 fps.

Figure 7: DYCAST Analysis of Seat Rail under Vertical Dynamic Loading
Length = 14 in. Load = 104 lbm at 30 fps.

Figure 8: DYCAST Analysis of Seat Rail under Vertical Dynamic Loading
Length = 18 in. Load = 104 lbm at 30 fps.

541

Figure 9: DYCAST Analysis of Seat Rail under Vertical Dynamic Loading
Length = 26 in. Load = 104 lbm at 30 fps.

Figure 10: DYCAST Analysis of Seat Rail under Vertical Dynamic Loading
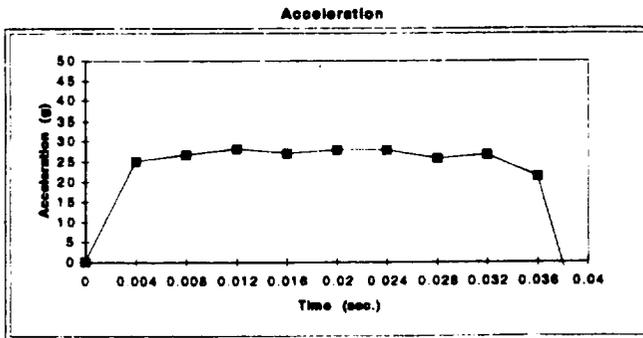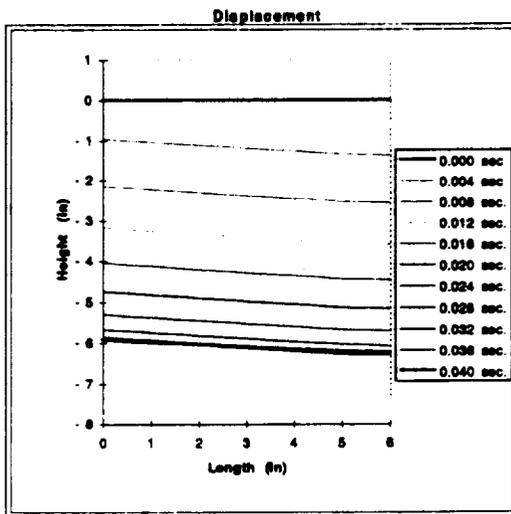Length = 36 in. Load = 104 lbm at 30 fps

Figure 11: DYCAST Analysis of Seat Rail under Vertical Dynamic Loading
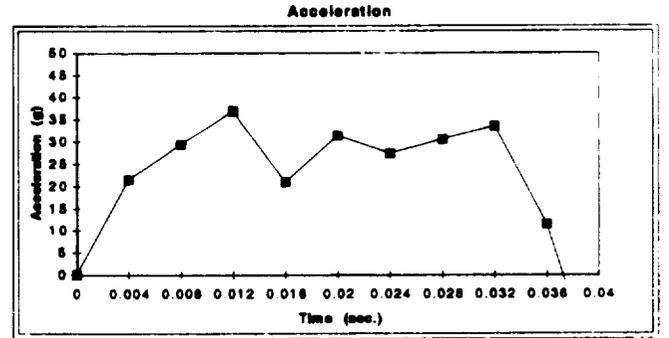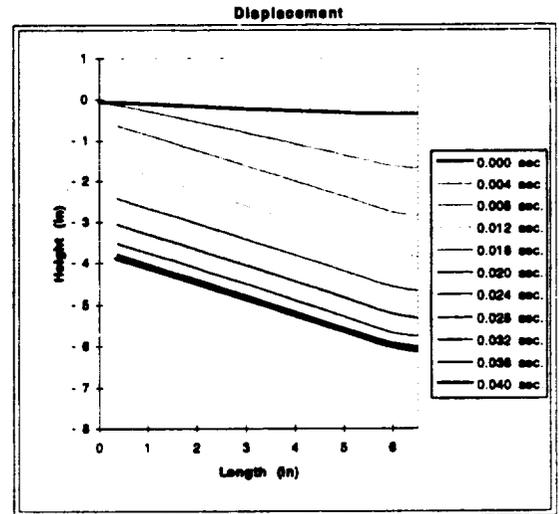Length = 12 in. Load = 104 lbm at 30 fps. Ends restrained.

Figure 12: DYCAST Analysis of Seat Rail under Vertical Dynamic Loading
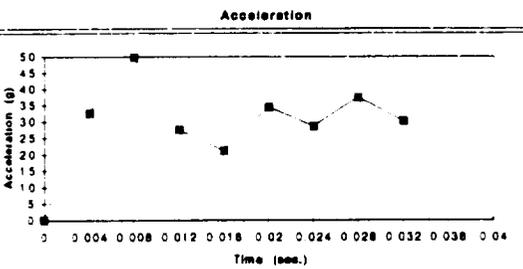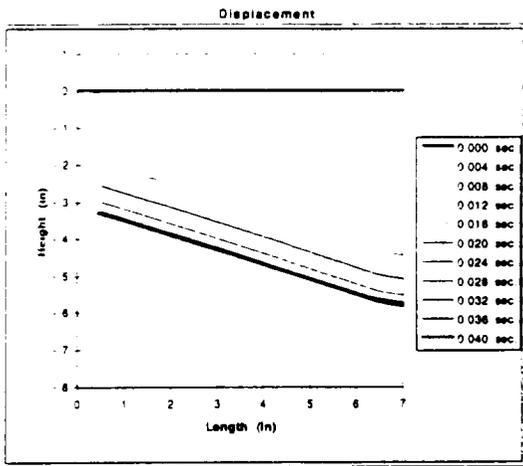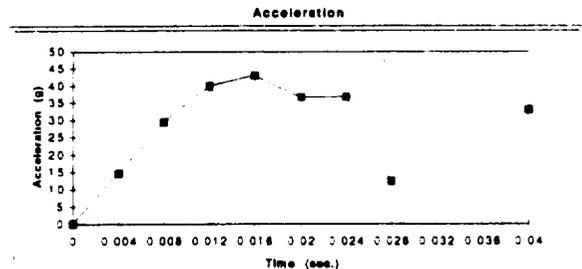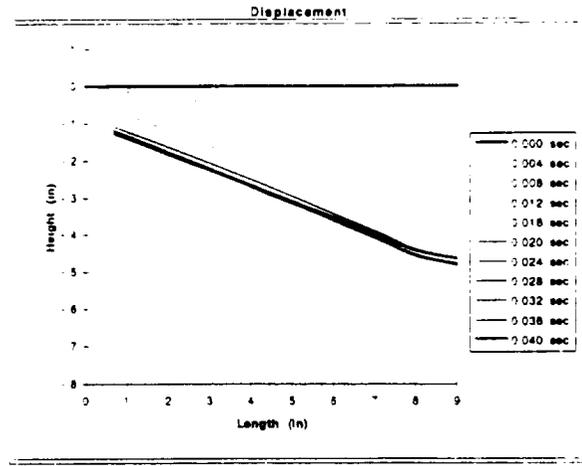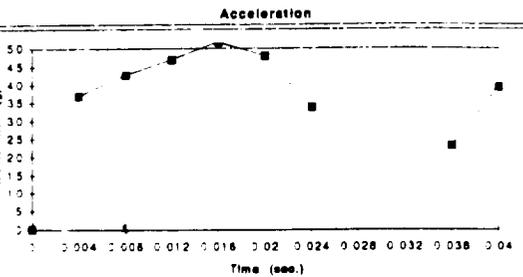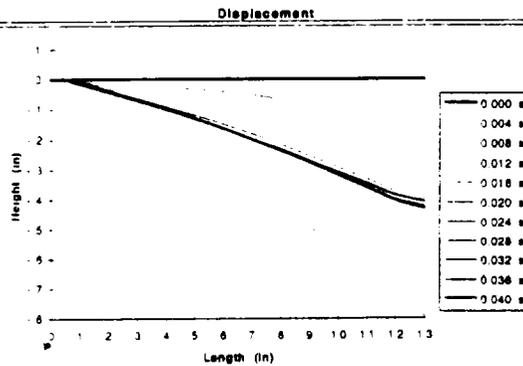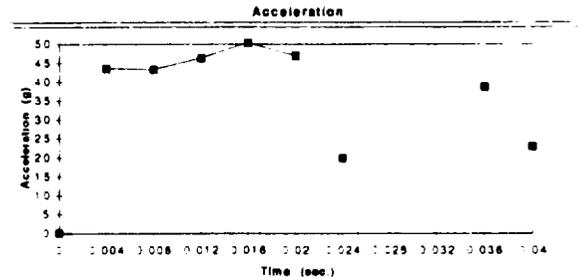Length = 13 in. Load = 104 lbm at 30 fps. Ends restrained.

Displacement

Height (in)

Length (in)

Legend:
- 0.000 sec
- 0.004 sec
- 0.008 sec
- 0.012 sec
- 0.016 sec
- 0.020 sec
- 0.024 sec
- 0.028 sec
- 0.032 sec
- 0.036 sec
- 0.040 sec

Acceleration

Acceleration (g)

Time (sec.)

Figure 13: DYCAST Analysis of Seat Rail under Vertical Dynamic Loading
Length = 14 in. Load = 104 lbm at 30 fps. Ends restrained.

Displacement

Height (in)

Length (in)

Legend:
- 0.000 sec
- 0.004 sec
- 0.008 sec
- 0.012 sec
- 0.016 sec
- 0.020 sec
- 0.024 sec
- 0.028 sec
- 0.032 sec
- 0.036 sec
- 0.040 sec

Acceleration

Acceleration (g)

Time (sec.)

Figure 14: DYCAST Analysis of Seat Rail under Vertical Dynamic Loading
Length = 18 in. Load = 104 lbm at 30 fps. Ends restrained

Displacement

Height (in)

Length (in)

Legend:
- 0.000 sec
- 0.004 sec
- 0.008 sec
- 0.012 sec
- 0.016 sec
- 0.020 sec
- 0.024 sec
- 0.028 sec
- 0.032 sec
- 0.036 sec
- 0.040 sec

Acceleration

Acceleration (g)

Time (sec.)

Figure 15: DYCAST Analysis of Seat Rail under Vertical Dynamic Loading
Length = 26 in. Load = 104 lbm at 30 fps. Ends restrained

Displacement

Height (in)

Length (in)

Legend:
- 0.000 sec
- 0.004 sec
- 0.008 sec
- 0.012 sec
- 0.016 sec
- 0.020 sec
- 0.024 sec
- 0.028 sec
- 0.032 sec
- 0.036 sec
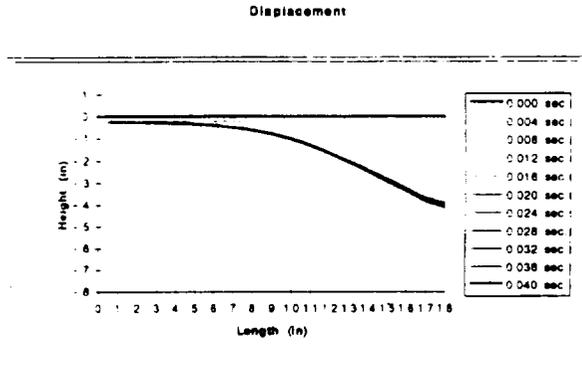- 0.040 sec

Acceleration

Acceleration (g)

Time (sec.)

Figure 16: DYCAST Analysis of Seat Rail under Vertical Dynamic Loading
Length = 36 in. Load = 104 lbm at 30 fps. Ends restrained

543